Activated IL-6 signaling contributes to the pathogenesis of, and is a novel therapeutic target for, *CALR*-mutated MPNs

Manjola Balliu,[1,2] Laura Calabresi,[1,2] Niccolò Bartalucci,[1,2] Simone Romagnoli,[1-3] Laura Maggi,[4] Rossella Manfredini,[5] Matteo Lulli,[6] Paola Guglielmelli,[1,2] and Alessandro Maria Vannucchi[1,2]

[1]Center of Research and Innovation of Myeloproliferative Neoplasms (CRIMM), Department of Experimental and Clinical Medicine, University of Florence, Florence, Italy; [2]DENOTHE Excellence Center, Azienda Ospedaliera Universitaria Careggi, Florence, Italy; [3]GENOMEC Doctorate School, University of Siena, Siena, Italy; [4]Department of Experimental and Clinical Medicine, University of Florence, Florence, Italy; [5]Center for Regenerative Medicine, Department of Life Sciences, University of Modena and Reggio Emilia, Modena, Italy; and [6]Department of Experimental and Clinical Biomedical Sciences "Mario Serio," University of Florence, Florence, Italy

Key Points

- Cells harboring the MPN-associated CALR mutation show cell-autonomous activation of the IL-6 pathway.

- Inhibition of IL-6 signaling may have therapeutic potential in MPNs.

Calreticulin (CALR), an endoplasmic reticulum–associated chaperone, is frequently mutated in myeloproliferative neoplasms (MPNs). Mutated CALR promotes downstream JAK2/STAT5 signaling through interaction with, and activation of, the thrombopoietin receptor (MPL). Here, we provide evidence of a novel mechanism contributing to *CALR*-mutated MPNs, represented by abnormal activation of the interleukin 6 (IL-6)-signaling pathway. We found that UT7 and UT7/mpl cells, engineered by clustered regularly interspaced short palindromic repeats (CRISPR)/CRISPR-associated protein 9 (Cas9) to express the *CALR* type 1–like (DEL) mutation, acquired cytokine independence and were primed to the megakaryocyte (Mk) lineage. Levels of *IL-6* messenger RNA (mRNA), extracellular-released IL-6, membrane-associated glycoprotein 130 (gp130), and IL-6 receptor (IL-6R), phosphorylated JAK1 and STAT3 (p-JAK1 and p-STAT3), and IL-6 promoter region occupancy by STAT3 all resulted in increased *CALR* DEL cells in the absence of MPL stimulation. Wild-type, but not mutated, CALR physically interacted with gp130 and IL-6R, downregulating their expression on the cell membrane. Agents targeting gp130 (SC-144), IL-6R (tocilizumab [TCZ]), and cell-released IL-6 reduced proliferation of *CALR* DEL as well as *CALR* knockout cells, supporting a mutated CALR loss-of-function model. CD34+ cells from *CALR*-mutated patients showed increased levels of *IL-6* mRNA and p-STAT3, and colony-forming unit–Mk growth was inhibited by either SC144 or TCZ, as well as an IL-6 antibody, supporting cell-autonomous activation of the IL-6 pathway. Targeting IL-6 signaling also reduced colony formation by CD34+ cells of JAK2V617F-mutated patients. The combination of TCZ and ruxolitinib was synergistic at very low nanomolar concentrations. Overall, our results suggest that target inhibition of IL-6 signaling may have therapeutic potential in *CALR,* and possibly *JAK2*V617F, mutated MPNs.

Introduction

Calreticulin (CALR) is a 46-kDa multicompartmental, prevalently endoplasmic reticulum (ER)-associated protein that regulates cellular responses important in wound healing, fibrosis, immune response, and cancer.[1] The protein has 3 domains: the N-terminal domain, with chaperone activity; a central proline-rich (P) domain that has chaperone activity and binds calcium with high affinity; and a C-terminal domain that contains low-affinity, high-capacity calcium-binding sites and terminates with an ER

The full-text version of this article contains a data supplement.

retention/retrieval motif (KDEL).[2] Within the ER lumen, CALR ensures proper folding of proteins and glycoproteins, and controls protein quality by preventing protein aggregation and facilitating progression of misfolded proteins to ubiquitin-mediated destruction.[3] CALR knockout (KO) is lethal during embryogenesis due to defective heart development.[4]

Somatic mutations of CALR occur in 70% to 80% of patients with essential thrombocythemia and primary myelofibrosis (PMF) who lack JAK2V617F and MPL canonical mutations.[5,6] CALR mutations are typically heterozygous, and involve the last protein exon, encoding for most of the C terminus. CALR mutations consist of >50 indel variants; of these, >80% are classified as type 1 (a 52-bp deletion, L367fs*46; DEL) and type 1–like, based on predicted helical secondary structure,[7] or type 2 (a 5-bp insertion, K385fs*47; INS) and type 2–like.[8,9] All CALR mutations create a +1-bp frameshift in exon 9 resulting in a novel C terminus. Type 1 mutations eliminate all negatively charged exon 9 amino acids, whereas some negatively charged amino acids remain in type 2 mutations, possibly accounting for differences in calcium-binding impairment; notably, the clinical phenotype is usually more severe in the type 1 mutation.[9-12]

The CALR mutation is detected in the long-term hematopoietic stem cell compartment, representing an early oncogenic event in the pathogenesis of CALR^mut myeloproliferative neoplasms (MPNs). Animal models confirmed that expression of mutated CALR is sufficient to induce an MPN manifesting with thrombocytosis that, although not invariably, progresses to myelofibrosis.[13-16] Recent studies showed that mutated CALR binds to the thrombopoietin (TPO) receptor (MPL) in the ER and on the outside of the cell, resulting in MPL aberrant activation.[17-19] MPL engagement induces downstream activation of JAK/STAT signaling[20]; notably, splenomegaly reduction and symptomatic improvement were noted in CALR^mut patients who received the JAK2/JAK1 inhibitor ruxolitinib, similar to patients with JAK2V617F or MPL mutation.[21] However, prominent activation of the MAPK pathway in CALR^mut cells was also reported.[22]

Expression of CALR in normal CD34^+ cells increases as they differentiate to megakaryocytes (Mks)[23]; these findings, and the engagement of MPL by mutated CALR, may explain the prevalent involvement of the Mk lineage in CALR^mut diseases. However, owing to the broad action of CALR in protein and calcium homeostasis, it is hypothesized that additional mechanisms may contribute to the phenotype of CALR^mut MPNs. To address this point, we analyzed different cellular models, engineered by clustered regularly interspaced short palindromic repeats (CRISPR)/CRISPR-associated protein 9 (Cas9) genome editing to express CALR DEL, or with target deletion (KO) of CALR, as well as primary cells from CALR^mut patients, and provide evidence that mutated CALR is involved in abnormal activation of the interleukin 6 (IL-6) pathway.

Methods

Cell lines and primary CD34^+ cell culture

The granulocyte macrophage–colony-stimulating factor (GM-CSF)-dependent UT7 (Deutsche Sammlung von Mikroorganismen und Zellkulturen [DSMZ]) and GM-CSF and TPO-dependent UT7/mpl cells (kindly donated by W. Vainchenker, INSERM, Unité Mixte de Recherche, Institut Gustave Roussy, Villejuif, France) were routinely passed with GM-CSF. CD34^+ cells were magnetically isolated from healthy donors' cord blood (CB) and the blood and bone marrow of CALR- and JAK2V617F-mutated patients (see supplemental Table 1 for patient characteristics). Collection and processing of human samples was approved by the Azienda Ospedaliera-Universitaria Careggi Institutional Review Board (#14560) after obtaining informed written consent.

CRISPR/Cas9 gene editing and transfection

We generated CALR KO cells from CB CD34^+ cells, UT7 and UT7/mpl cell lines, and CALR type 1 (DEL) variants from UT7 and UT7/mpl cells. To obtain KO variants, cells were transfected with pCMV-Cas9-GFP plasmid together with a guide sequence complementary to CALR exon 1. To generate DEL variants, cells were transfected with the pCMV-Cas9-GFP plasmid, a pU6 plasmid containing the guide RNA sequence complementary to a stretch of genomic DNA and an additional single-strand donor oligonucleotide allowing the knock-in of the specific mutation by homology-directed repair. Single green fluorescent protein–positive (GFP^+) cells were sorted into individual wells of a 96-well plate. Individual clones were validated using polymerase chain reaction (PCR), Sanger sequencing, quantitative reverse transcription PCR (qRT-PCR), and western blot. For CRISPR/Cas9 genome editing of CB CD34^+, GFP^+ transfected cells were bulk sorted into a tube containing the appropriate medium. Transient overexpression of CALR wild-type (WT) and CALR DEL was obtained by transfecting UT7/mpl CALR KO cells with the following plasmids: p-CMV3-(N)Flag-CALR WT, p-CMV3-(N)Flag-CALR DEL, and an empty vector as control. Standard methods for DNA/RNA purification, Sanger sequencing, and qRT-PCR were used.

Cell proliferation and apoptosis measurements

An automated trypan blue dye exclusion system was used for enumerating live cells; cell-cycle distribution was determined by propidium iodide and apoptosis by annexin V/propidium iodide staining, followed by flow cytometry.

Induced Mk differentiation

UT7/mpl cells were induced to Mk differentiation without/with TPO for 7 days. Mk differentiation was assessed by CD41-phycoerythrin and CD61–fluorescein isothiocyanate expression with flow cytometry.

Flow cytometry analysis of CD41/CD61 expression

Standard methodology was used with appropriate, labeled antibodies, on unfixed cells.

Colony assays of primary hematopoietic progenitors

CD34^+ cells were plated in cytokine-supplemented methylcellulose, for burst-forming unit erythroid (BFU-E) and colony-forming unit (CFU) granulocyte macrophage (CFU-GM), and collagen medium, for CFU-Mk generation.

Protein analysis

Immunoblot and immunoprecipitation was performed following standard methodology. Quantification of interleukin 6 (IL-6) in culture supernatants was performed using an enzyme-linked immunosorbent assay (ELISA) technique.

ChIP assay

The chromatin immunoprecipitation (ChIP) assay was performed using a commercially available ChIP assay kit. Immunoprecipitation of *CALR* WT, DEL, and KO UT7 and UT7/mpl cell extracts to assess IL-6 promoter region chromatin occupancy by STAT3 was performed with STAT3 antibody. The primers used for the PCR following ChIP are listed in supplemental Methods.

Confocal microscopy

Confocal microscopy was performed according to standard methodology, using glycoprotein 130 (gp130), IL-6 receptor (IL-6R), and phospho-STAT3 (p-STAT3) antibodies.

Statistical analysis

The Student *t* test or 1-way analysis of variance were used as appropriate; the *P* value was fixed at ≤.05.

A full description of methods and reagents is provided as supplemental Methods.

Results

Development and characterization of CRISPR/Cas9-edited *CALR* DEL and KO cell lines

We generated *CALR* DEL and KO UT7 and UT7/mpl cell lines by CRISPR/Cas9 technology. We generated a frameshift in *CALR* exon 9 gene, resulting in a STOP codon and the transcription of a type 1–like protein (now *CALR* DEL cells). The mutant clones were characterized by Sanger sequencing (Figure 1A), qRT-PCR, and western blotting. UT7 and UT7/mpl *CALR* DEL cells expressed mutated CALR of the expected size and sequence, lacking the KDEL motif (Figure 1B). We noticed faint expression levels of DEL CALR across several different clones analyzed (not shown in detail), despite *CALR* messenger RNA (mRNA) levels being comparable to WT parental cells (Figure 1B), suggesting that mutated protein is less stable than WT protein, as reported.[22,24] *CALR* KO cells were obtained by either disruption of start codon ATG (UT7 cells) or introduction of a STOP codon in exon 1 (UT7/mpl cells) resulting in no CALR protein expression (Figure 1A-B).

Under standard cytokine-supplemented culture conditions, the proliferation rate (supplemental Figure 1) of parental, *CALR* DEL, and KO cell lines was no different; however, *CALR* DEL and KO UT7 and UT/mpl cells showed extended survival and resistance to apoptosis, compared with parental cells, when cultured under cytokine depletion (Figure 1C-D). These findings indicated that *CALR* DEL cells expressing mutant CALR acquired cytokine independence to a certain extent, and this effect was phenocopied by a *CALR* KO condition.

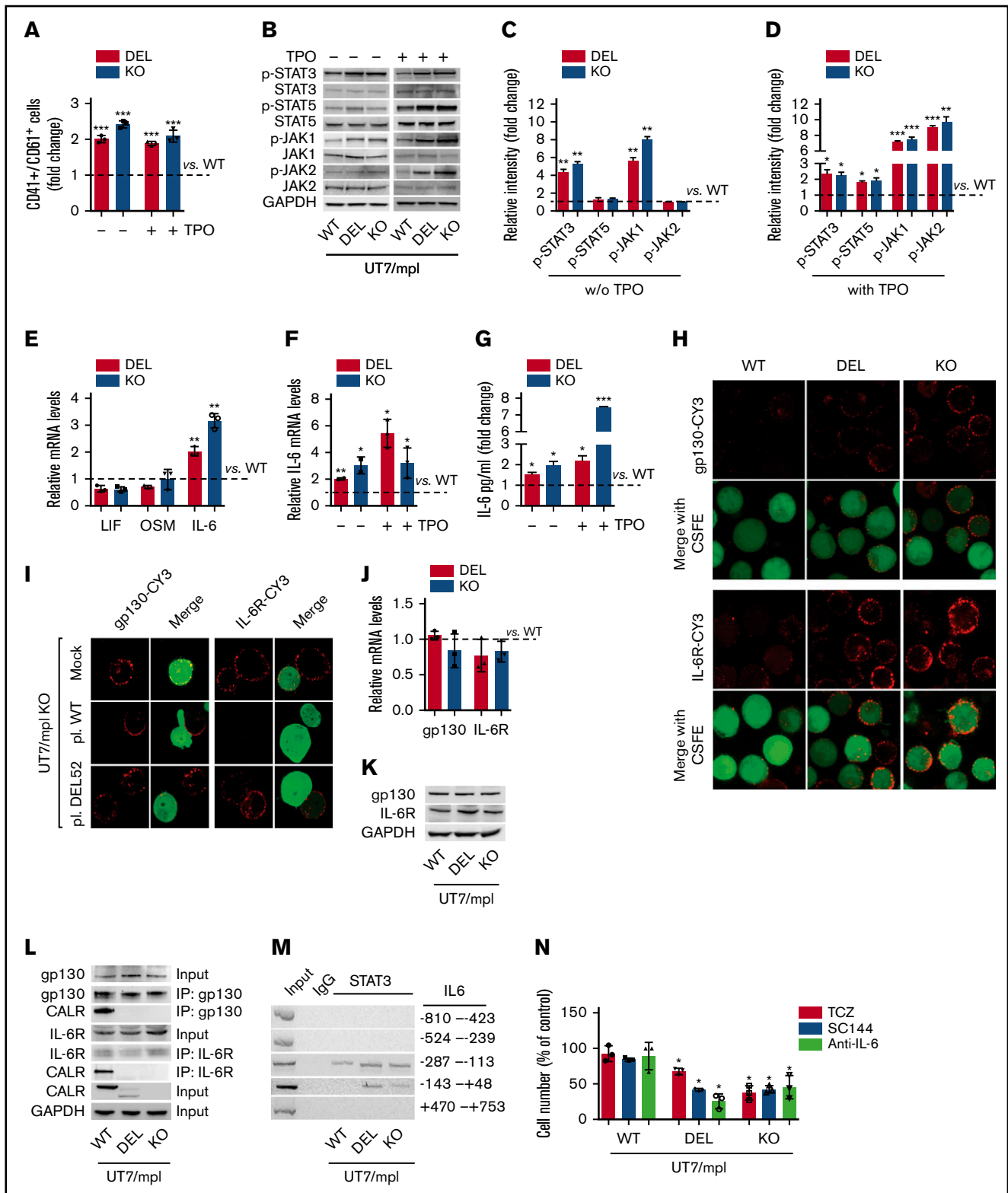### The IL-6–signaling pathway is abnormally activated in *CALR* DEL and KO mutant cells

Several studies reported preferential involvement of the Mk cell lineage in patients harboring the *CALR* mutation,[10,17,22,23,25,26] associated with activation of JAK2/STAT5 signaling.[17] To this end, we first assessed TPO-induced and TPO-independent megakaryocytic differentiation of *CALR* DEL and KO UT7/mpl cells. After 7 days of culture with TPO, CD41$^+$/CD61$^+$ cells increased by 1.9-fold and 2.1-fold, respectively, in *CALR* DEL and KO cells compared with WT cells (*P* < .001; Figure 2A); notably,

CD41$^+$/CD61$^+$ cells were similarly increased (2.0-fold and 2.4-fold, respectively, vs controls) also in TPO-deprived conditions. In the latter cell culture conditions, we observed increased p-JAK1 and p-STAT3 levels in both *CALR* DEL and KO cells[24] (5.6-fold and 7.95-fold and 4.3-fold and 5.3-fold, respectively, in a typical experiment in Figure 2B), whereas p-JAK2 and p-STAT5 were similar to WT cells. However, in *CALR* DEL cells exposed to TPO, p-JAK1 (7.2-fold), p-JAK2 (9.1-fold), p-STAT3 (2.3-fold), and p-STAT5 (1.8-fold) were all upregulated in comparison with WT cells; similar changes were observed in *CALR* KO cells (7.5-fold, 10-fold, 2.2-fold, and 1.9-fold, respectively) (mean plus or minus standard deviation [SD] densitometric values of 3 experiments are shown in Figure 3C-D). These findings suggested that *CALR* DEL mutation and lack of WT protein induced autonomous, TPO-independent activation of JAK1/STAT3 signaling, whereas JAK2/STAT5 signaling was preferentially induced by activation of MPL in either *CALR* DEL or KO cells. Because members of the IL-6 family are among the most important activators of STAT3,[27] we investigated the mRNA levels of selected members of this family in *CALR* DEL and KO UT7/mpl cells. In standard culture conditions without TPO, *IL-6* mRNA levels were 2.0-fold and 3.2-fold, respectively, higher in *CALR* DEL and KO cells than parental cells, whereas *LIF* and *OSM* mRNA levels were unchanged (Figure 2E) and *IL11* mRNA was below the detection limit (not shown). The *IL-6* mRNA levels were further increased in UT7/mpl cells exposed to TPO (from 2.0-fold and 3.0-fold the controls in *CALR* DEL and KO cells in the absence of TPO to 5.5-fold and 3.2-fold, respectively, when cultured with TPO; Figure 2F), consistent with known JAK2-dependent activation of *IL-6* transcription. Increased amounts of IL-6 were released in the culture medium of *CALR* DEL and KO UT7/mpl cells maintained without or with TPO (1.5-fold ± 0.1-fold and 2.0-fold ± 0.2-fold, and 2.2-fold ± 0.2-fold and 7.4-fold ± 0.1-fold, vs controls, respectively) (Figure 2G). We also investigated the expression of gp130 and IL-6R on the cell membrane by confocal microscopy, finding that they were expressed at higher levels in CALR DEL and KO UT7/mpl cells compared with WT cells (Figure 2H), confirmed by flow cytometry (supplemental Figure 2). Then, we transiently expressed WT and DEL CALR in *CALR* KO cells, finding that expression of gp130 or IL-6R receptors was overtly reduced in cells expressing the WT, unlike DEL, CALR (Figure 2I). These findings, together with the appreciation that mRNA levels (Figure 2J) and total protein content of gp130 and IL-6R (Figure 2K) in *CALR* DEL and KO cells was similar to WT counterparts, supported the hypothesis that increased membrane expression of gp130 and IL-6R is due to abnormal processing of the receptors by mutated CALR, an effect phenocopied by absence of WT protein in KO cells. Therefore, WT CALR might be physiologically involved in negative regulation of gp130 and IL-6R expression on the cell membrane. In support of that, we demonstrated direct interaction of WT CALR, but not the DEL variant, with IL-6R and gp130 by coimmunoprecipitation experiments (Figure 2L); CALR–IL-6 immunocomplexes were not detected.

Finally, we performed a ChIP assay to analyze occupancy of candidate STAT3-binding sites in the IL-6 promoter[28]; we found evidence of enhanced interaction of STAT3 at region −238 to −113 and particularly −143 to +48 in *CALR* DEL and KO cells compared with parental cells (Figure 2M). Moreover, as the promoter of IL-6 contains both NF-κB and STAT3-binding sites,

Figure 1. Development and characterization of *CALR* DEL and KO cell lines. (A) The strategy to obtain *CALR* KO (targeting exon 1) and DEL (targeting exon 9) UT7 and UT7/mpl cell lines with CRISPR/Cas9 genome editing; the resulting DNA sequence of genome-edited clones used in the study is reported below the sequence of WT *CALR*, or a typical del52 mutation, at corresponding DNA regions of interest for KO and DEL targeting. The ATG start codon is in bold and underlined; in the UT7 KO cell line, the ATG is removed whereas in UT7/mpl, the KO conditions were due to insertion of a TAG stop codon (in bold and red). The predicted sequence of the resulting DEL protein for UT7 and UT7/mpl is shown within a rectangle, with the novel sequence in red and the common C terminus underlined. (B) The expression of *CALR* mRNA and CALR protein in *CALR* WT (parental), DEL and KO UT7, and UT7/mpl cell lines was assessed, respectively, by qRT-PCR (top panel) and western blotting (bottom panel), using antibodies to either the common N-terminal or the C-terminal KDEL domain. Glyceraldehyde-3-phosphate dehydrogenase (GAPDH) was used for loading normalization; the asterisk points to mutant protein. (C-D) The GM-CSF–dependent UT7 and TPO-dependent UT7/mpl cells, either parental, *CALR* DEL, or KO, were seeded at 2×10^5 cells per milliliter in cytokine-free medium. Living cells ($\times 10^5$/mL) were counted daily by trypan blue dye exclusion (top panels). Cell apoptosis was assessed at day 3 using the Annexin V–Fluoassay, and expressed as the percentage of annexin V$^+$ cells over total (for UT7 [E] and UT7/mpl [F] cell lines, respectively). Data are the mean plus or minus SD of 3 independent experiments. All *P* values were determined by Student *t* test (*$P < .05$; **$P < .01$; ***$P < .001$).

NF-κB was also investigated. We did not find a significant modulation in terms of expression and activation of NF-κB in *CALR* DEL and KO cells compared with the WT counterpart (supplemental Figure 3).

Because these findings pointed to involvement of the IL-6 pathway in cells either expressing mutated CALR or lacking WT protein, we exploited the effects of different inhibitors of this pathway. We found that SC144, a chemical inhibitor of gp130, tocilizumab (TCZ), an IL-6R–blocking monoclonal antibody, and a monoclonal anti–IL-6 antibody, all significantly reduced proliferation of *CALR* DEL and KO UT7/mpl cells, leaving parental cells largely unaffected

(Figure 2N). At day 3 of culture, *CALR* DEL and KO cells were reduced, respectively, by 58.3% ± 1.2% and 57.2% ± 3.6% when exposed to SC144, 33.4% ± 3.1% and 62.6% ± 7.2% with TCZ, and 74.1% ± 3.4% and 54.4% ± 5.5% with anti–IL-6 antibody, compared with untreated cells.

IL-6–signaling pathway activation in *CALR* DEL and KO mutant cells is independent of MPL expression

To rule out any possible interference of MPL-dependent JAK/ STAT5 activation on the autonomous activation of the IL-6 pathway in *CALR*-mutated cells, we repeated key experiments with UT7 cells that do not express the TPO receptor. We found that: (i) *IL-6* mRNA

Figure 2. CALR regulates IL-6/JAK1/STAT3 signaling through interaction with IL-6 and gp130. (A) UT7/mpl cells were incubated with TPO (100 ng/mL) or without for 7 days and the percentage of CD41$^+$/CD61$^+$ cells was measured by flow cytometry. Data shown are the mean plus SD of at least 3 individual experiments and represent fold change compared with WT cells incubated in the same conditions. (B) Total cell extracts of *CALR* WT, DEL, and KO UT7/mpl cells, incubated with or without TPO, were subjected to western blotting and immunodetection for p-STAT3, STAT3, p-STAT5, STAT5, p-JAK1, JAK1, p-JAK2, and JAK2; GAPDH was used as the loading control. (C-D) Densitometric analysis of 3 individual immunoblots (cells without TPO [C]) and (cells incubated with TPO [D]). *LIF*, *OSM*, and *IL-6* mRNA levels were measured by qRT-PCR in *CALR* DEL and KO UT7/mpl cells and expressed relative to WT cells (dashed line). (E) *RNAseP* mRNA levels were used for relative quantity (RQ) calculation. (F) The *IL-6*
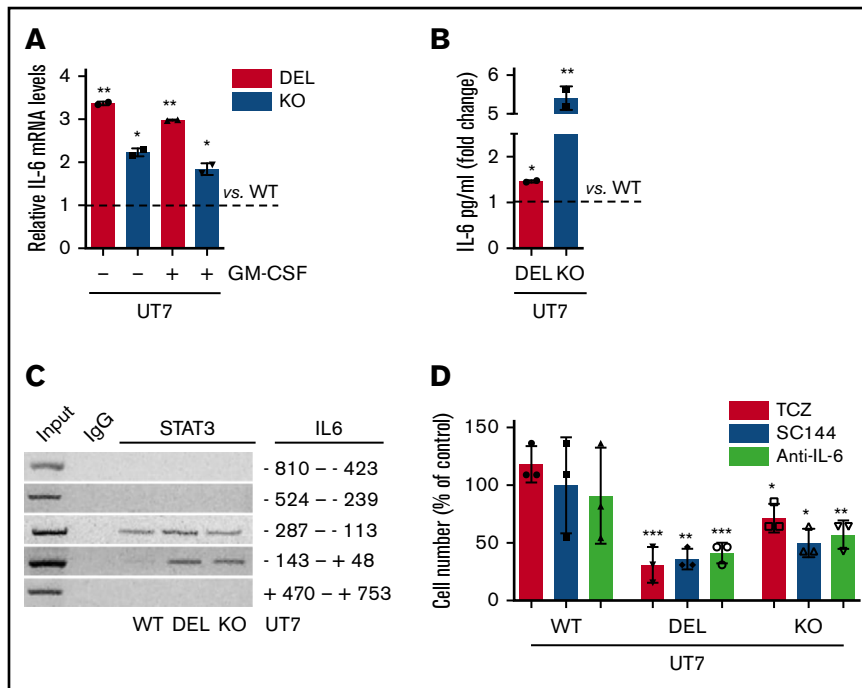
Figure 3. Abnormal IL-6 pathway activation is independent of MPL. (A) The *IL-6* mRNA levels were measured by qRT-PCR in *CALR* DEL and KO UT7 cells grown in the presence or absence of GM-CSF and expressed relative to *CALR* WT cells (dashed line). *RNAseP* mRNA levels were used for relative quantity (RQ) calculation. The levels of IL-6 in the culture medium of *CALR* DEL and KO UT7 cells were quantified by ELISA and expressed as fold change relative to parental cells (dashed line; panel B). (C) ChIP assay was performed in extracts of *CALR* WT, DEL, and KO UT7 cells using STAT3 antibody, or normal rabbit serum (IgG) as negative control, with the primers amplifying the indicated regions of the IL-6 promoter. (D) *CALR* WT, DEL, and KO UT7 cells were seeded at 1×10^5 cells per milliliter, in the presence of TCZ (1 μg/mL), SC144 (5 μM), and anti–IL-6 antibody (1 μg/mL), and living cells were counted daily by trypan blue dye exclusion; data shown represent percent changes compared with respective control cells maintained in the absence of drugs, for 3 days of culture, and are the mean plus or minus SD of 3 independent experiments. All *P* values were determined by Student *t* test (*P < .05; **P < .01; ***P < .01).

levels were increased in *CALR* DEL and KO cells compared with parental cells, irrespective of being exposed or not to GM-CSF, used to support cell survival and proliferation (3.0-fold and 1.8-fold, and 3.4-fold and 2.2-fold, respectively; Figure 3A); (ii) the amount of IL-6 released in the culture medium of *CALR* DEL and KO UT7 cells was 1.5-fold ± 0.1-fold and 5.4-fold ± 0.2-fold higher than parental

cells (Figure 3B); (iii) STAT3 protein bound to the promoter of IL-6 in *CALR*-mutated UT7 cells (Figure 3C): finally, UT7 *CALR* DEL and KO cell proliferation was significantly inhibited after exposure to IL-6 pathway inhibitors (Figure 3D). At day 3 of culture, *CALR* DEL and KO UT7 cells were reduced, respectively, by 63.9% ± 3% and 50% ± 4.1% when exposed to SC144, 69.1% ± 5.2% and 28.6%

Figure 2. (continued) mRNA levels were also measured in *CALR* WT (reference fixed to relative level 1, dashed line), DEL and KO UT7/mpl cells that were cultured in the presence or absence of TPO in culture medium. (G) The quantification by ELISA of the levels of IL-6 in the culture medium of *CALR* DEL and KO UT7/mpl cells, expressed relative to parental cells (dashed line). (H) The expression of IL-6R and gp130 on the cell membrane of *CALR* WT, DEL, and KO UT7/mpl cells was assessed by confocal microscopy. Carboxyfluorescein succinimidyl ester (CSFE) dye was used to identify living cells; original magnification ×200. (I) In these experiments, *CALR* KO UT7/mpl cells were transfected with *CALR* WT-GFP– and *CALR* DEL-GFP–expressing plasmids (pl.), then they were challenged with antibodies (red fluorescence) against membrane-associated gp130 (left panels) and IL-6R (right panels). In the "merge" fields, green fluorescence points to cells that were successfully transfected with the expression plasmid; cells labeled with antibody only (red fluorescence) and lacking green fluorescence denote baseline expression of either gp130 or IL-6R in KO cells that were not transfected. Representative cells in confocal microscopy fields are presented to illustrate changes of receptor expression on the membrane of GFP-transfected KO cells; original magnification ×200. (J-K) The levels of gp130 and IL-6R mRNA (J; expressed relative to WT cells, dashed line) and protein in total cell extracts (K) were assessed by qRT-PCR and western blot, respectively, in *CALR* DEL and KO UT7/mpl cells; GAPDH was used for loading normalization. (L) In the coimmunoprecipitation experiment shown (1 representative of at least 3 for each experimental condition), whole-cell extracts of *CALR* WT, DEL, and KO cells were immunoprecipitated with gp130 (top) and IL-6R (bottom) antibodies and revealed with respective antibodies and CALR N-terminal antibody. Input panels represent the quantification of respective proteins in whole extracts before immunoprecipitation. (M) ChIP assay was performed in extracts of *CALR* WT, DEL, and KO UT7/mpl cells using STAT3 antibody, or normal rabbit serum (immunoglobulin G [IgG]) as negative control, with the primers amplifying the indicated regions of the IL-6 promoter. (N) *CALR* WT, DEL, and KO UT7/mpl cells were seeded at 2×10^5 cells per milliliter, in cytokine-free medium, and living cells were counted daily by trypan blue dye exclusion; data shown are at day 3 of culture and are expressed as percent change compared with respective control cell cultures in the absence of drug. TCZ (1 μg/mL), a monoclonal anti–IL-6R antibody, SC144 (5 μM), a small molecule inhibitor of gp130, and anti–IL-6 antibody (1 μg/mL), were added at the initiation of culture (chosen drug concentrations were predetermined in dose-response curves). Data are expressed as the mean plus or minus SD of 3 independent experiments. All *P* values were determined by Student *t* test (*P < .05; **P < .01; ***P < .01).
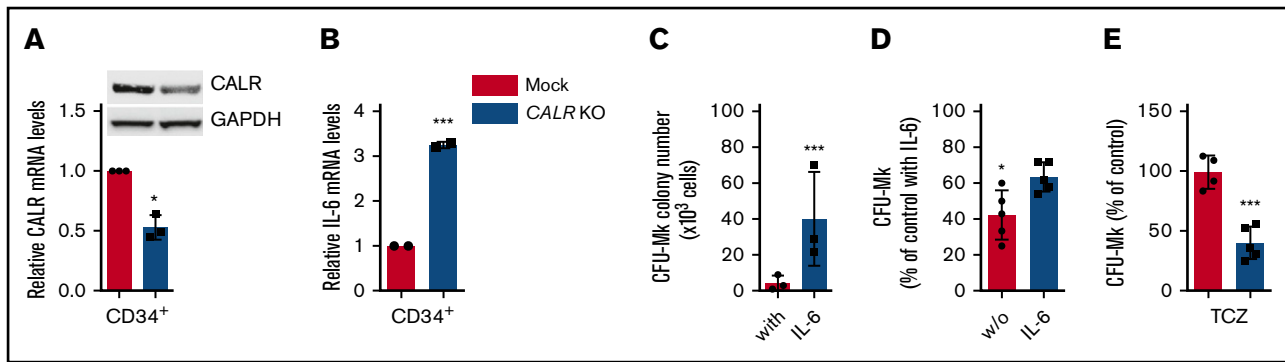
Figure 4. Downregulation of WT CALR in normal CD34⁺ cells increases IL-6–dependent CFU-Mk generation. (A) Immunopurified CD34⁺ cells from donor CB units were transfected with a *CALR* CRISPR-GFP plasmid targeting exon 1 to generate a KO condition, or a mock CRISPR-GFP plasmid; cells were sorted based on high fluorescence intensity and analyzed for *CALR* mRNA (by qRT-PCR) and protein (by western blotting) expression levels. *CALR* mRNA levels are expressed relative to *RNAseP* mRNA levels, used for relative quantity (RQ) calculation. In these same cell preparations, the levels of *IL-6* mRNA were measured by qRT-PCR, and expressed relative to WT cells, set at value 1 (panel B). (C-E) CRISPR-edited CD34⁺ cells were sorted based on their high GFP expression and plated in clonogenic plasma clot cultures for growth of CFU-Mk colonies, in the presence (C) or absence (D) of IL-6 in the culture medium. (E) In these experiments, cells were cultured in the absence of IL-6 but in the presence of TCZ (5 ng/mL). Data for each experimental condition represent the mean plus SD of at least 3 experiments. All *P* values were determined by Student *t* test (*$P < .05$; ***$P < .001$).

± 4.1% with TCZ, and 58.8% ± 3% and 42.9% ± 4.1% with anti–IL-6 antibody, compared with controls.

These findings support MPL-independent activation of IL-6 signaling due to dysregulated exposure of gp130 and IL-6R on the cell membrane and STAT3-mediated IL-6 overproduction, caused by loss of a regulatory function exerted by WT CALR on IL-6 receptor processing.

CRISPR/Cas9-induced haploinsufficiency of WT CALR in normal CD34⁺ cells increases IL-6–dependent CFU-Mk generation

Aimed at validating the observations herein in primary cells, we first manipulated CB-derived CD34⁺ cells with a CRISPR/Cas9/GFP plasmid targeting exon 1, to induce a *CALR* KO condition; cells treated with mock CRISPR/Cas9/GFP plasmid served as control. Conversely, we were unable to generate *CALR* DEL cells due to low efficiency of the CRISPR/Cas9 DEL plasmid in CD34⁺ cells. Sorted CD34⁺ cells according to the highest GFP levels displayed ~50% reduction of CALR mRNA and protein content, compared with mock cells, compatible with a heterozygous KO condition (Figure 4A). *IL-6* mRNA levels were increased by 3.2-fold + 0.3-fold in *CALR* KO CD34⁺ vs mock cells ($P < .001$; Figure 4B). When sorted *CALR* KO CD34⁺ cells were plated in plasma clot cultures containing IL-6, CFU-Mks were 10-fold higher than the mock counterpart (from 4.3 ± 1.4 to 40.1 ± 8.7/10³ plated cells; $P < .001$; Figure 4C); furthermore, in the IL-6–deprived condition, the anticipated reduction of CFU-MK generated from *CALR* KO CD34⁺ cells was lower than untouched cells (38.2% + 4.3% vs 58.0% + 13.1%; $P < .05$; Figure 4D). Finally, the addition of IL-6R inhibitor TCZ significantly reduced the number of CFU-Mk colonies generated from *CALR* KO CD34⁺ cells ($P < .001$) by 57.1% ± 2.7%, whereas mock CD34⁺ were largely unaffected (Figure 4E). Overall, these findings indicate that a condition of functional haploinsufficiency of CALR in CD34⁺ cells is associated with abnormal activation of IL-6 signaling contributing to enhanced megakaryocytopoiesis in vitro.

CFU-Mk colony generation in vitro from *CALR*- and *JAK2*V617F-mutated patients is synergistically inhibited by JAK1/2 and the IL-6R inhibitor

To ascertain the role of IL-6 signaling in *JAK2*V617F-mutated patients, we compared CFU-Mks generated from CD34⁺ cells of *CALR*- and *JAK2*V617F-mutated patients. In IL-6–supplemented medium, the number of CFU-Mk colonies per 10³ CD34⁺ cells plated was 30.7 ± 1.3, 45.6 ± 5.6, and 13.1 ± 2.6 for *JAK2*V617F-mutated, *CALR*-mutated, and control subjects, respectively. The deprivation of IL-6 from culture medium caused a significant reduction (−34.6% ± 2.8%; $P < .01$) of CFU-Mks from control CD34⁺ cells, unlike *CALR* mutant or *JAK2*V617F patients (−5.2% ± 1.0% and −1.90% ± 2.4%; Figure 5A). *IL-6* mRNA levels in CD34⁺ cells were 9.9-fold and 10.6-fold higher in *CALR*- and *JAK2*V617F-mutated patients than controls ($P < .01$; Figure 5B). We also found that the majority (70% ± 10%) of CD34⁺ cells of *CALR*- and *JAK2*V617F-mutated patients showed bright p-STAT3 immunofluorescence compared with a minority (<5%) of control CD34⁺ cells (Figure 5C). Increased expression of gp130 and IL-6R on CD34⁺ cells from *CALR*- and *JAK2*V617F-mutated patients was confirmed by flow cytometry; CD34⁺gp130⁺ cells were 32.7% ± 1.6%, 42.4% ± 1.3%, and 22.9% ± 1.2%, and CD34⁺ IL-6R⁺ cells were 28.3% ± 2.7%, 29.5% ± 1.3%, and 13% ± 0.6%, in *CALR* mutated, *JAK2*V617F mutated, and controls, respectively (Figure 5D-E). Also, the gp130 and IL-6R mean fluorescent intensity was 1.4-fold and 1.6-fold in *CALR*-mutated cells, and 1.6-fold and 1.4-fold in *JAK2*V617F-mutated cells, higher than control cells. (Figure 5F-G). As a whole, these findings suggested autonomously activated IL-6 signaling in CD34⁺ cells of *CALR*- and *JAK2*V617F-mutated patients.

In clonogenic assays established with *CALR*- and *JAK2*V617F-mutated CD34⁺ cells, we found dose-dependent inhibition of CFU-Mk generation, unlike in control plates. The 50% inhibitory concentration (IC50) for CFU-Mks in cultures of CD34⁺ cells from *CALR*- and *JAK2*V617F-mutated patients was, respectively, 4.3 ± 0.2 nM and 8.1 ± 3.1 nM for SC144, 69.5 ± 7.8 ng/mL and
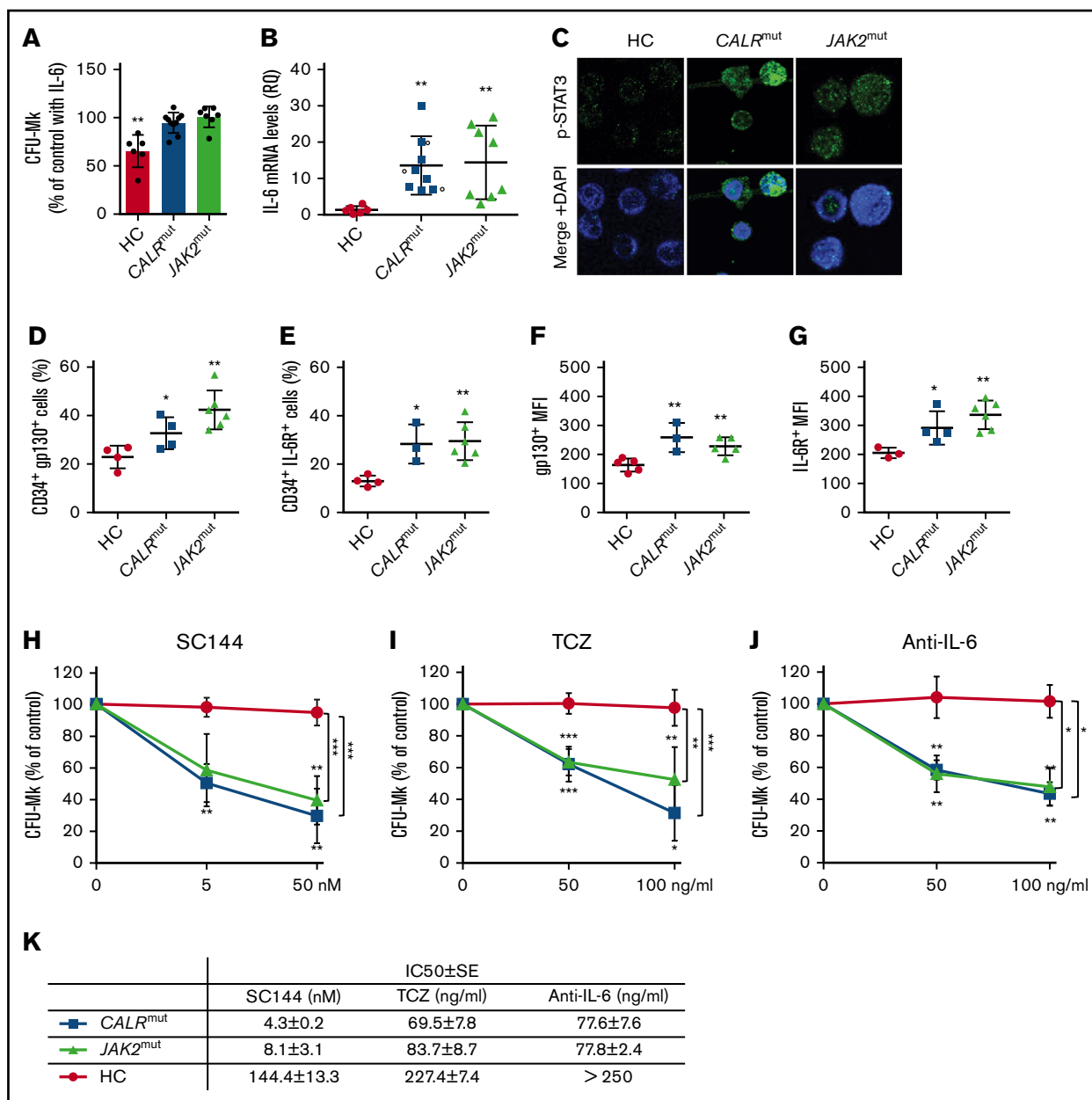
Figure 5. CFU-Mk generation from CD34$^+$ cells of *CALR*- and *JAK2*V617F-mutated patients is dependent on IL-6. Immunomagnetically isolated CD34$^+$ cells from healthy controls (HC; n = 6), *CALR*-mutated (n = 10), or *JAK2*V617F-mutated (n = 7) patients were seeded in MegaCult medium depleted of IL-6; CFU-Mk colonies were counted on day 12. Data are expressed as percent of control cultures in media containing IL-6 (A). The levels of *IL-6* mRNA were assessed by qRT-PCR in CD34$^+$ cells from *CALR*- (n = 8) and *JAK2*V617F-mutated (n = 8) MPN patients and healthy controls (HC; n = 7). Data are expressed as relative quantity (RQ) to reference *RNAseP* mRNA. (B) The symbol ° points to 3 *CALR* type 2–mutated patients, whereas the remaining 5 were typical DEL mutation. (C) The expression of p-STAT3 was evaluated by confocal microscopy in isolated CD34$^+$ cells from *CALR*- or *JAK2*V617F-mutated patients or healthy subjects (n = 3 for each category; ×200 magnification). Random chosen cells from 1 healthy control, *CALR*- or *JAK2*V617F-mutated patient are presented. DAPI (4′,6-diamidino-2-phenylindole) dye was used to identify the nucleus. (D-G) The expression of gp130 and IL-6R on the cell membrane of *CALR*^{mut}, *JAK2*V617F^{mut} patients and healthy controls was assessed by flow cytometry; the percentage of positive cells (D-E) and the mean fluorescent intensity (F-G) are shown. (H-J) Dose-dependent inhibition of CFU-Mk generation in clonogenic cultures established from *CALR*-mutated (n = 6) or *JAK2*V617F-mutated (n = 5) patients and healthy controls (HC; n = 6). SC144, TCZ, and an anti–IL-6 antibody were added at the time of culture initiation. CFU-Mk colonies from triplicate dishes were counted after 12 days, and the number of colonies was expressed as percent of controls in the absence of respective drugs. Respective IC50 values (mean plus standard error [SE]) are detailed in panel K. All *P* values were determined by Student *t* test (*$P < .05$; **$P < .01$; ***$P < .001$).

83.7 ± 8.7 ng/mL for TCZ, and 77.6 ± 2.5 ng/mL and 77.7 ± 2.4 ng/mL for anti–IL-6 antibody (Figure 5H-K). We also evaluated the effects of IL-6 pathway inhibitors in clonogenic cultures for CFU-GM and BFU-E (supplemental Figure 4). We found that TCZ at 250 ng/mL inhibited the number of CFU-GM generated by *CALR*- and *JAK2*V617F-mutated CD34$^+$ cells by 51.67% ± 5.8%
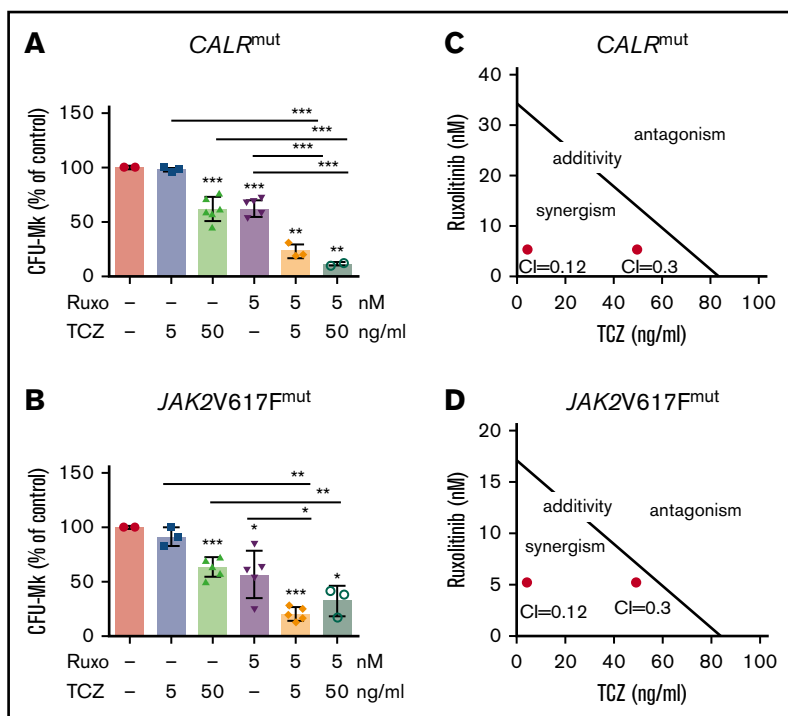
Figure 6. Combination of TCZ and ruxolitinib synergistically inhibits CFU-Mk generation from *CALR*- and *JAK2*V617F-mutated patients. (A-B) CD34^{+} isolated from *CALR*-mutated (n = 4) and *JAK2*V617F-mutated (n = 5) patients, respectively, were plated in IL-6–free clonogenic assays for CFU-Mk generation. Ruxolitinib (Ruxo; at a suboptimal dose of 5 nM) and TCZ (at 5 and 50 ng/mL) were added at the initiation of culture, and CFU-Mks were counted on day 12. Data are shown as percent number of colonies to control cultures in the absence of either drug. The isobologram for IC50 of TCZ and ruxolitinib to inhibiting CFU-Mk generation in *CALR*[mut] (C) and *JAK2*V617F[mut] (D) patients was calculated according to the Chou and Talalay formula. All *P* values were determined by the Student *t* test (*$P < .05$; **$P < .01$; ***$P < .001$).

and 48.34% ± 5.1%; SC144 was similarly effective with 47.5% ± 1.9% and 48.9% ± 1.8% inhibition at 100 nM. TCZ was minimally effective on BFU-E, with a 33.2% ± 3.4% and 17.5% ± 3.2% reduction in *CALR*- and *JAK2*V617F-mutated patients at 250 ng/mL, whereas SC144 were more effective: at 100 nM, the number of BFU-E generated by *CALR*- and *JAK2*V617F-mutated CD34^{+} was reduced by 84.7% ± 5.4% and 48.3% ± 2.8%, respectively.

We finally ascertained whether the combination of TCZ and ruxolitinib resulted in synergistic inhibition of CFU-Mk generation; to this end, we used suboptimal amounts of ruxolitinib (5 nM) and TCZ (5 and 50 ng/mL). We found that CFU-Mks were reduced, respectively, by 70.8% ± 2.0% and 90.8% ± 0.7% (from 30.5 ± 2.2 to 8.9 ± 0.6 and 2.8 ± 1.1/10^3 plated cells; Figure 6A) in cultures of *CALR*-mutated CD34^{+} cells, and by 79.5% ± 1.2% and 64.1% ± 4.5% (from 45.7 ± 4.9 to 9.3 ± 2.0 and 16.4 ± 6.8/10^3 plated cells; Figure 6B) from *JAK2*V617F cells, resulting in respective combination indexes of 0.12 and 0.30 (Figure 6C-D).[29]

Discussion

CALR mutation is detected in 20% to 25% of essential thrombocythemia and PMF patients who show unique characteristics compared with *JAK2*V617F mutated.[30-33] The best known mechanism for mutated CALR in MPN pathogenesis is through its abnormal binding and activation of the TPO receptor MPL, which is expressed on hematopoietic stem cells and the megakaryocytic lineage. Activated MPL insists on JAK2/STAT5 signaling, as in *JAK2*V617F-mutated cells, as well as on the MAPK pathway.[22,34] The activation of JAK-dependent cascade justifies the clinical benefits of JAK2/JAK1 inhibitor ruxolitinib and fedratinib in *CALR*[mut] patients.[21,35]

We present herein data supporting a novel mode of action of mutated CALR. Using UT7 and UT7/mpl cells CRISPR/Cas9

engineered to express *CALR* type I–like DEL mutation, we showed that cells acquire cytokine independence, become primed for Mk differentiation, express raised *IL-6* mRNA and extracellularly released IL-6 levels, with higher membrane-associated gp130 and IL-6R, and increased levels of p-JAK1 and p-STAT3; these were all independent of MPL stimulation by TPO. Of note, these effects were reproduced in UT7 and UT7/mpl cells made KO for *CALR*. We also showed that WT CALR, but not mutated CALR, physically interacts with gp130 and IL-6R. Accordingly, we propose that WT CALR physiologically limits the exposure of gp130 and IL-6R on the cell membrane, compatible with a loss of function of mutated CALR, phenocopied by CALR KO. Mutated CALR was shown to be similarly involved in the transport of immature, or traffic-defective, MPL from the ER to the cell membrane.[19,36] The augmented membrane exposure of IL-6Rs would in turn promote *IL-6* transcription through increased occupancy of the IL-6 promoter by STAT3, resulting in a feed-forward autocrine feedback loop.[37,38] We also showed that CB CD34^{+} cells engineered to become haploinsufficient for WT *CALR*, as well as primary CD34^{+} cells isolated from *CALR*[mut] patients (including a few with *CALR* type 2 mutation), presented increased expression of *IL-6* mRNA and dependence on autocrine IL-6 for CFU-Mk generation. Furthermore, we showed that agents targeting gp130 (SC144) or IL-6R (TCZ) inhibited the growth of *CALR* DEL/KO cells and, more importantly, Mk colonies from CD34^{+} progenitors of *CALR*[mut] patients; such inhibition was synergistically potentiated by ruxolitinib, raising the provoking perspective that these 2 approved agents may be efficaciously combined in vivo. TCZ is a humanized antibody that competitively inhibits IL-6 binding to its receptor; it is approved for the treatment of rheumatoid arthritis, chimeric antigen receptor-T-cell–induced cytokine release syndrome, and idiopathic multicentric Castleman disease.[38,39] The effective concentrations of TCZ in cultures of CD34^{+} cells in our experiments were in the low range of 5 to 100 ng/mL, well within the steady-state peak and

through concentration (183 + 86 µg/mL and 9.7 + 1.1 µg/mL, respectively) of a clinically used dose of 8 mg/kg.[40]

When activated by IL-6, the intracytoplasmic portion of IL-6R binds to gp130, triggering receptor dimerization and signal transduction via either the JAK/STAT or MAPK pathway.[39] IL-6 acts directly by inducing the expression of STAT3 target genes, which among the others encode proteins that drive tumor cell proliferation (such as cyclin D1) and survival (such as BCL-xL).[38,41] IL-6 is normally involved in megakaryocytopoiesis in both TPO-dependent and TPO-independent mechanisms.[42,43] Therefore, it makes sense that *IL-6* mRNA levels were increased also in CD34$^+$ cells of *JAK2*V617F^{mut} patients, owing to autonomous activation of JAK2 signaling, and that inhibitors of IL-6 signaling and extracellularly released IL-6 inhibited CFU-Mk generation. However, the effects of blocking IL-6 signaling may extend beyond the Mk lineage, as supported by TCZ-induced inhibition of myeloid (CFU-GM) progenitors, and to lower extent, erythroid ones, of *CALR*^{mut} and *JAK2*V617F^{mut} patients.

Intriguingly, circulating CALR was found to be associated with IL-6 plasma levels and disease severity in patients with MF.[44] It is also noteworthy that in a mouse chronic myelogenous leukemia model, abnormal production of IL-6 by leukemic stem cells sustained leukemia development; conceivably, disease-associated spleno-megaly and myeloid expansion in hematopoietic tissues were abrogated by anti–IL-6 antibody.[45] Kleppe et al identified IL-6 as one of the most abnormally produced inflammatory cytokines by granulocytes of PMF patients that was associated with constitutive STAT3 activation. Pan-hematopoietic Stat3 deletion in the context of an MPL^{W515L} MPN mouse model resulted in amelioration of the myelofibrosis trait, consistent with a requirement of STAT3 in malignant and nonmalignant hematopoietic cells.[46] Furthermore, a loss-of-function polymorphism of IL-6R (rs4537545) was associated with reduced risk of developing a *JAK2*V617F^{mut} MPN in a Danish population study.[47] Dual targeting of JAK2 and STAT3 (via IL-6R blockade) may therefore have attractiveness for the treatment of MPN patients.[48,49] Using the same reasoning, targeting NF-κB with BET bromodomain protein inhibitors, alone and in combination with ruxolitinib, was therapeutically effective in MPN models and post-MPN acute leukemia cells.[48,50]

As a whole, our data support an abnormal interaction between mutated CALR and gp130 and IL-6R. As pointed out in an elegant commentary by Ann Mullally,[51] the complexity of the role of mutated CALR is broadening from "gains," exemplified by its well-characterized interaction with MPL, to "losses," including defective interaction with ERp57, a member of the protein disulfide isomerase family involved in calcium regulation,[52] deficiency of myeloperox-idase in leukocytes,[53] and abnormal processing of IL-6 receptors, according to data presented in this manuscript. This concept is strengthened by findings that mutated CALR was faithfully phenocopied by absence (UT7 and UT7/mpl KO cells) or haploinsufficiency of WT (CD34$^+$ KO cells). Theocharides et al

observed that deficiency of myeloperoxidase was mostly pronounced in leukocytes of patients harboring homozygous *CALR* mutation,[53] and Shide et al recently demonstrated that CALR haploinsufficiency in hematopoietic cell–specific Calr-deficient mice was necessary for the onset of myeloproliferation, and augmented stem cell activity.[54]

Though providing compelling in vitro and ex vivo evidence to support IL-6 as a novel pathogenetic mechanism and therapeutic target for *CALR*- and, possibly, *JAK2*V617F-mutated MPN, this study poses some questions that deserve to be investigated in future experiments. The first regards whether the therapeutic efficacy of combined JAK2/IL-6 inhibition will be substantiated in in vivo models; absence of animal data are an acknowledged limitation of current work. An additional aspect to explore is whether paracrine effects might also contribute to abnormal IL-6 pathway activation in MPN hematopoietic cells, as inflammatory cytokines originate both from the MPN clone as well as nonclonal cells.

Authorship

Contribution: M.B., L.C., N.B., and P.G. designed the research and analyzed data; S.R., L.M., and M.L. contributed to experimental data; R.M. contributed to analysis; and A.M.V. designed the research and wrote the paper with the collaboration of P.G. and M.B.

Conflict-of-interest disclosure: A.M.V. is on the advisory board for Novartis, Celgene, AbbVie, Incyte, Italfarmaco, and CTI; and is a speaker for Novartis, Celgene, and CTI. P.G. is on the advisory board of, and is a speaker for, Novartis. The remaining authors declare no competing financial interests.

ORCID profiles: N.B., 0000-0002-9328-3948; S.R., 0000-0001-5744-3716; L.M., 0000-0003-2862-9591; R.M., 0000-0003-0660-6110; M.L., 0000-0002-8528-4094; P.G., 0000-0003-1809-284X; A.M.V., 0000-0001-5755-0730.

Correspondence: Alessandro M. Vannucchi, CRIMM, Centro di Ricerca e Innovazione e Laboratorio Congiunto per le Malattie Mieloproliferative, AOU Careggi, Dipartimento di Medicina Sperimentale e Clinica and DENOTHE Excellence Center, CUBO 3, Padiglione 27b, Viale Pieraccini, 6, 50134 Firenze, Italy; e-mail: amvannucchi@unifi.it.

References

1. Lu Y-C, Weng W-C, Lee H. Functional roles of calreticulin in cancer biology. *BioMed Res Int*. 2015;2015:526524.

2. Gold LI, Eggleton P, Sweetwyne MT, et al. Calreticulin: non-endoplasmic reticulum functions in physiology and disease. *FASEB J*. 2010;24(3):665-683.

3. Kozlov G, Gehring K. Calnexin cycle - structural features of the ER chaperone system. *FEBS J*. 2020;287(20):4322-4340.

4. Mesaeli N, Nakamura K, Zvaritch E, et al. Calreticulin is essential for cardiac development. *J Cell Biol*. 1999;144(5):857-868.

5. Nangalia J, Massie CE, Baxter EJ, et al. Somatic CALR mutations in myeloproliferative neoplasms with nonmutated JAK2. *N Engl J Med*. 2013;369(25):2391-2405.

6. Klampfl T, Gisslinger H, Harutyunyan AS, et al. Somatic mutations of calreticulin in myeloproliferative neoplasms. *N Engl J Med*. 2013;369(25):2379-2390.

7. Tefferi A, Lasho TL, Tischer A, et al. The prognostic advantage of calreticulin mutations in myelofibrosis might be confined to type 1 or type 1-like CALR variants. *Blood*. 2014;124(15):2465-2466.

8. Tefferi A, Wassie EA, Guglielmelli P, et al. Type 1 versus type 2 calreticulin mutations in essential thrombocythemia: a collaborative study of 1027 patients. *Am J Hematol*. 2014;89(8):E121-E124.

9. Tefferi A, Lasho TL, Finke C, et al. Type 1 vs type 2 calreticulin mutations in primary myelofibrosis: differences in phenotype and prognostic impact. *Leukemia*. 2014;28(7):1568-1570.

10. How J, Hobbs GS, Mullally A. Mutant calreticulin in myeloproliferative neoplasms. *Blood*. 2019;134(25):2242-2248.

11. Guglielmelli P, Rotunno G, Fanelli T, et al. Validation of the differential prognostic impact of type 1/type 1-like versus type 2/type 2-like CALR mutations in myelofibrosis [letter]. *Blood Cancer J*. 2015;5(10):e360.

12. Guglielmelli P, Lasho TL, Rotunno G, et al. MIPSS70: mutation-enhanced International Prognostic Score System for transplantation-age patients with primary myelofibrosis. *J Clin Oncol*. 2018;36(4):310-318.

13. Marty C, Pecquet C, Nivarthi H, et al. Calreticulin mutants in mice induce an MPL-dependent thrombocytosis with frequent progression to myelofibrosis. *Blood*. 2016;127(10):1317-1324.

14. Li J, Prins D, Park HJ, et al. Mutant calreticulin knockin mice develop thrombocytosis and myelofibrosis without a stem cell self-renewal advantage. *Blood*. 2018;131(6):649-661.

15. Balligand T, Achouri Y, Pecquet C, et al. Knock-in of murine Calr del52 induces essential thrombocythemia with slow-rising dominance in mice and reveals key role of Calr exon 9 in cardiac development. *Leukemia*. 2020;34(2):510-521.

16. Benlabiod C, Cacemiro MDC, Nédélec A, et al. Calreticulin del52 and ins5 knock-in mice recapitulate different myeloproliferative phenotypes observed in patients with MPN. *Nat Commun*. 2020;11(1):4886.

17. Chachoua I, Pecquet C, El-Khoury M, et al. Thrombopoietin receptor activation by myeloproliferative neoplasm associated calreticulin mutants. *Blood*. 2016;127(10):1325-1335.

18. Elf S, Abdelfattah NS, Chen E, et al. Mutant calreticulin requires both its mutant C-terminus and the thrombopoietin receptor for oncogenic transformation. *Cancer Discov*. 2016;6(4):368-381.

19. Pecquet C, Chachoua I, Roy A, et al. Calreticulin mutants as oncogenic rogue chaperones for TpoR and traffic-defective pathogenic TpoR mutants. *Blood*. 2019;133(25):2669-2681.

20. Balligand T, Achouri Y, Pecquet C, et al. Pathologic activation of thrombopoietin receptor and JAK2-STAT5 pathway by frameshift mutants of mouse calreticulin. *Leukemia*. 2016;30(8):1775-1778.

21. Guglielmelli P, Rotunno G, Bogani C, et al; COMFORT-II Investigators. Ruxolitinib is an effective treatment for CALR-positive patients with myelofibrosis. *Br J Haematol*. 2016;173(6):938-940.

22. Kollmann K, Warsch W, Gonzalez-Arias C, et al. A novel signalling screen demonstrates that CALR mutations activate essential MAPK signalling and facilitate megakaryocyte differentiation. *Leukemia*. 2017;31(4):934-944.

23. Vannucchi AM, Rotunno G, Bartalucci N, et al. Calreticulin mutation-specific immunostaining in myeloproliferative neoplasms: pathogenetic insight and diagnostic value. *Leukemia*. 2014;28(9):1811-1818.

24. Pronier E, Cifani P, Merlinsky TR, et al. Targeting the CALR interactome in myeloproliferative neoplasms. *JCI Insight*. 2018;3(22):e122703.

25. Kollmann K, Nangalia J, Warsch W, et al. MARIMO cells harbor a CALR mutation but are not dependent on JAK2/STAT5 signaling. *Leukemia*. 2015;29(2):494-497.

26. Vainchenker W, Kralovics R. Genetic basis and molecular pathophysiology of classical myeloproliferative neoplasms. *Blood*. 2017;129(6):667-679.

27. Heinrich PC, Behrmann I, Müller-Newen G, Schaper F, Graeve L. Interleukin-6-type cytokine signalling through the gp130/Jak/STAT pathway. *Biochem J*. 1998;334(Pt 2):297-314.

28. Yoon S, Woo SU, Kang JH, et al. NF-κB and STAT3 cooperatively induce IL6 in starved cancer cells. *Oncogene*. 2012;31(29):3467-3481.

29. Chou T-C. Drug combination studies and their synergy quantification using the Chou-Talalay method. *Cancer Res*. 2010;70(2):440-446.

30. Rotunno G, Mannarelli C, Guglielmelli P, et al; Associazione Italiana per la Ricerca sul Cancro Gruppo Italiano Malattie Mieloproliferative Investigators. Impact of calreticulin mutations on clinical and hematological phenotype and outcome in essential thrombocythemia. *Blood*. 2014;123(10):1552-1555.

31. Rumi E, Pietra D, Pascutto C, et al; Associazione Italiana per la Ricerca sul Cancro Gruppo Italiano Malattie Mieloproliferative Investigators. Clinical effect of driver mutations of JAK2, CALR, or MPL in primary myelofibrosis. *Blood*. 2014;124(7):1062-1069.

32. Tefferi A, Nicolosi M, Mudireddy M, et al. Driver mutations and prognosis in primary myelofibrosis: Mayo-Careggi MPN alliance study of 1,095 patients. *Am J Hematol*. 2018;93(3):348-355.

33. Guglielmelli P, Pacilli A, Rotunno G, et al; AGIMM Group. Presentation and outcome of patients with 2016 WHO diagnosis of prefibrotic and overt primary myelofibrosis. *Blood*. 2017;129(24):3227-3236.

34. Fu C, Wen QJ, Marinaccio C, et al. AKT activation is a feature of CALR mutant myeloproliferative neoplasms. *Leukemia*. 2019;33(1):271-274.

35. Passamonti F, Caramazza D, Maffioli M. JAK inhibitor in CALR-mutant myelofibrosis. *N Engl J Med*. 2014;370(12):1168-1169.

36. Masubuchi N, Araki M, Yang Y, et al. Mutant calreticulin interacts with MPL in the secretion pathway for activation on the cell surface. *Leukemia*. 2020; 34(2):499-509.

37. Chang Q, Bournazou E, Sansone P, et al. The IL-6/JAK/Stat3 feed-forward loop drives tumorigenesis and metastasis. *Neoplasia*. 2013;15(7):848-862.

38. Johnson DE, O'Keefe RA, Grandis JR. Targeting the IL-6/JAK/STAT3 signalling axis in cancer. *Nat Rev Clin Oncol*. 2018;15(4):234-248.

39. Uciechowski P, Dempke WCM. Interleukin-6: a masterplayer in the cytokine network. *Oncology*. 2020;98(3):131-137.

40. Zhang X, Peck R. Clinical pharmacology of tocilizumab for the treatment of patients with rheumatoid arthritis. *Expert Rev Clin Pharmacol*. 2011;4(5): 539-558.

41. Jones SA, Jenkins BJ. Recent insights into targeting the IL-6 cytokine family in inflammatory diseases and cancer. *Nat Rev Immunol*. 2018;18(12): 773-789.

42. Sui X, Tsuji K, Ebihara Y, et al. Soluble interleukin-6 (IL-6) receptor with IL-6 stimulates megakaryopoiesis from human CD34(+) cells through glycoprotein (gp)130 signaling. *Blood*. 1999;93(8):2525-2532.

43. Sim X, Poncz M, Gadue P, French DL. Understanding platelet generation from megakaryocytes: implications for in vitro-derived platelets. *Blood*. 2016; 127(10):1227-1233.

44. Sollazzo D, Forte D, Polverelli N, et al. Circulating calreticulin is increased in myelofibrosis: correlation with interleukin-6 plasma levels, bone marrow fibrosis, and splenomegaly. *Mediators Inflamm*. 2016;2016:5860657.

45. Welner RS, Amabile G, Bararia D, et al. Treatment of chronic myelogenous leukemia by blocking cytokine alterations found in normal stem and progenitor cells. *Cancer Cell*. 2015;27(5):671-681.

46. Kleppe M, Kwak M, Koppikar P, et al. JAK-STAT pathway activation in malignant and nonmalignant cells contributes to MPN pathogenesis and therapeutic response. *Cancer Discov*. 2015;5(3):316-331.

47. Pedersen KM, Çolak Y, Ellervik C, Hasselbalch HC, Bojesen SE, Nordestgaard BG. Loss-of-function polymorphism in IL6R reduces risk of JAK2V617F somatic mutation and myeloproliferative neoplasm: a Mendelian randomization study. *EClinicalMedicine*. 2020;21:100280.

48. Kleppe M, Koche R, Zou L, et al. Dual targeting of oncogenic activation and inflammatory signaling increases therapeutic efficacy in myeloproliferative neoplasms [published correction appears in *Cancer Cell*. 2018;33(4):785-787]. *Cancer Cell*. 2018;33(1):29-43.e7.

49. Pedersen KM, Çolak Y, Hasselbalch HC, Bojesen SE, Nordestgaard BG. Tocilizumab and soluble interleukin-6 receptor in JAK2V617F somatic mutation and myeloproliferative neoplasm [letter]. *EClinicalMedicine*. 2020;22:100337.

50. Saenz DT, Fiskus W, Manshouri T, et al. BET protein bromodomain inhibitor-based combinations are highly active against post-myeloproliferative neoplasm secondary AML cells. *Leukemia*. 2017;31(3):678-687.

51. Mullally A. Both sides now: losses and gains of mutant CALR. *Blood*. 2020;135(2):82-83.

52. Di Buduo CA, Abbonante V, Marty C, et al. Defective interaction of mutant calreticulin and SOCE in megakaryocytes from patients with myeloproliferative neoplasms. *Blood*. 2020;135(2):133-144.

53. Theocharides APA, Lundberg P, Lakkaraju AKK, et al. Homozygous calreticulin mutations in patients with myelofibrosis lead to acquired myeloperoxidase deficiency. *Blood*. 2016;127(25):3253-3259.

54. Shide K, Kameda T, Kamiunten A, et al. Calreticulin haploinsufficiency augments stem cell activity and is required for onset of myeloproliferative neoplasms in mice. *Blood*. 2020;136(1):106-118.